*Sensors and Materials*, Vol. 35, No. 1 (2023) 135–151
MYU Tokyo


S & M 3159

# Estimation of Forest Net Primary Production in Northeast China Using the Physiological Principles Predicting Growth Model Driven by Remote Sensing Data

Yanan Liu,[1,2*] Peng Gao,[1] Dandan Liu,[3] Mengxue Xu,[1] Yian Wang,[1] and Ran Chen[1]

[1]School of Geomatics and Urban Spatial Informatics, Beijing University of Civil Engineering and Architecture, No. 1 Zhanlanguan Road, Beijing 100044, China
[2]Key Laboratory of Urban Spatial Information, Ministry of Natural Resources, Beijing 102616, China
[3]School of Civil and Architecture Engineering, Panzhihua University, Panzhihua, Sichuan 617000, China

(Received December 13, 2022; accepted January 16, 2023)

***Keywords:*** 3-PG, NPP, remote sensing, process-based model, influence factors

Accurately estimating net primary production (NPP) for various forest types on a large scale is of great significance to the global carbon cycle and climate change, particularly in terms of monthly variations. Most studies focus on the NPP estimation of individual tree species or a single forest type, and few studies explore the NPP estimation of multiple forest types simultaneously. Here, we aimed to explore the potential of the physiological principles predicting growth (3-PG) model to estimate the NPP of six typical tree species in Northeast China. Forest NPP was estimated on the basis of the 3-PG model using the fractional vegetation cover and leaf area index derived from moderate-resolution imaging spectroradiometer sensors. In addition, the monthly variation in forest NPP and factors influencing the NPP were analyzed. The results demonstrate that the proposed approach can yield reliable NPP estimates, and the determination coefficient (R2) between the estimated results and those obtained using the existing MODIS products was between 0.4010 and 0.5462. The forest NPP peaked approximately in July and was zero from October to April. Furthermore, the analysis of environmental effects on NPP indicated that temperature and site nutrition are the dominant forest growth factors, whereas available soil water is a limiting factor. Overall, we demonstrate that the proposed methodological framework satisfactorily estimated the NPP of the six typical tree species and has significant potential for forest growth prediction in China.

## 1. Introduction

As an important part of terrestrial ecosystems, forests have a strong carbon sink capacity and play an important role in the global carbon cycle.(1) Accurately assessing the carbon sequestration capacity of different forest types can help in the formulation of reasonable carbon sequestration strategies and provide services for protecting the standing stock of forest carbon pools and reducing the carbon emissions caused by deforestation and degraded forests. At present, the

*Corresponding author: e-mail: liuyanan@bucea.edu.cn
https://doi.org/10.18494/SAM4283

commonly used carbon sink estimation models include the climate productivity model, eco-physiological process model, light-use efficiency model, and coupling process model with remote sensing. Among them, remote-sensing-based methods have great potential for use in large-scale net primary production (NPP) estimation.

The climate productivity method mainly uses meteorological observations and NPP field surveys to build a regression model for forest NPP estimation. These models include the Miami,[2] Thomthwaite memorial,[3] and Chikugo[4] models. Although the climate productivity model is simple with easily obtainable parameters, its eco-physiological mechanism is unclear. The light-use efficiency model considers solar radiation and meteorological conditions to estimate the NPP. It can be easily transformed on a spatial scale, and dynamic monitoring results of the month, season, and year can be obtained. However, the physiological and ecological mechanisms of these models lack reliability. The eco-physiological process model can simulate the processes of photosynthesis, respiration, transpiration, and soil water loss in vegetation. By considering the atmosphere, vegetation, and soil as a unified ecosystem, it simulates the material and energy exchange processes in different layers by establishing different submodels. The process model has clear physiological and ecological mechanisms, and can simulate and predict the impact of global climate change on vegetation NPP. However, these models have certain limitations. For example, the structures of these models are complex, the parameters are numerous and difficult to obtain, and it is difficult to expand to large spatial scales. With the development of remote sensing technology, its advantages of being multisource and multiscale and the ability to extract forest ecological parameters will help solve the above problems.

The coupling process model with remote sensing combines the mechanism of the forest vegetation physiological growth process and ecological parameters derived from remote sensing data and can effectively transform the scale of forest vegetation parameters. At present, several NPP estimation methods use remote sensing data. Gong *et al.*[5] evaluated carbon fluxes from contemporary forest disturbances in North Carolina using a grid-based carbon accounting model and fine-resolution remote sensing products; Hazarika *et al.*[6] simulated NPP by combining the leaf area index (LAI) product obtained using MODIS sensors and the ecological process model, and the results indicated that the accuracy of NPP estimation depends on the reliability of the LAI. Zhou *et al.*[7] estimated the LAI using remote sensing data and estimated the NPP using the LAI and eco-physiological process model. Coupling a process model with remote sensing fully utilizes the spatial and temporal distribution information of remote sensing data and combines the physiological and ecological mechanisms of the process model to simulate and predict the vegetation NPP. However, the structure of the model is complex, and the accuracy of the estimation results is affected by ecological parameters derived from remote sensing data. Currently, significant differences remain in the spatial distribution and size of various NPP estimation models.

Although several studies have verified the NPP estimation models by comparatively analyzing the estimation results, no unified on appropriate verification method is currently available.[8] Productivity products are frequently used to evaluate NPP estimates. For example, mod17 [NPP and gross primary product (GPP)] derived from MODIS have been widely used to verify NPP estimation models. Zhang *et al.*[9] estimated the forest NPP by coupling the carbon exchange between vegetation, soil, and atmosphere (CEVSA) and global production efficiency models, and the estimated results were then compared and validated using mod17a3 NPP products.

Terrestrial ecosystems, especially forest ecosystems, in the middle and high latitudes of the Northern Hemisphere, play an important role as carbon sinks.(10) For example, Northeast China has the largest natural forest region in the country. The region has rich forest resources mainly distributed in the Daxing'an, Xiaoxing'an, and Changbai Mountains. Forest carbon storage and the capacity of carbon sinks play important roles in maintaining the national and regional carbon balance.(11) Therefore, estimating the forest NPP at the regional and national scales is highly important. The selected study site, Yichun City, is an important part of the ecological function area of Xiaoxing'an Mountain, which has rich forest resources.

## 2. Materials

### 2.1 Study site

The study site (Fig. 1) was Yichun City, Northeast China (46°28′–49°26′N, 127°37′–130°46′E). The terrain in the north is dominated by hills and platforms, the center is dominated by low hills and gentle slopes, and the south is dominated by low and steep hills. The study area, constituting an important ecological barrier with rich forest resources, has a north temperate continental monsoon climate with an annual average temperature between −1 and 1 °C, and a relatively short frost-free period (approximately 100–120 days). The highest monthly average temperature is between 20 and 22 °C. The total forest area covers greater than 3 million hectares with the coverage rate exceeding 80%. The forests are dominated by Korean pine (*Pinus koraiensis*

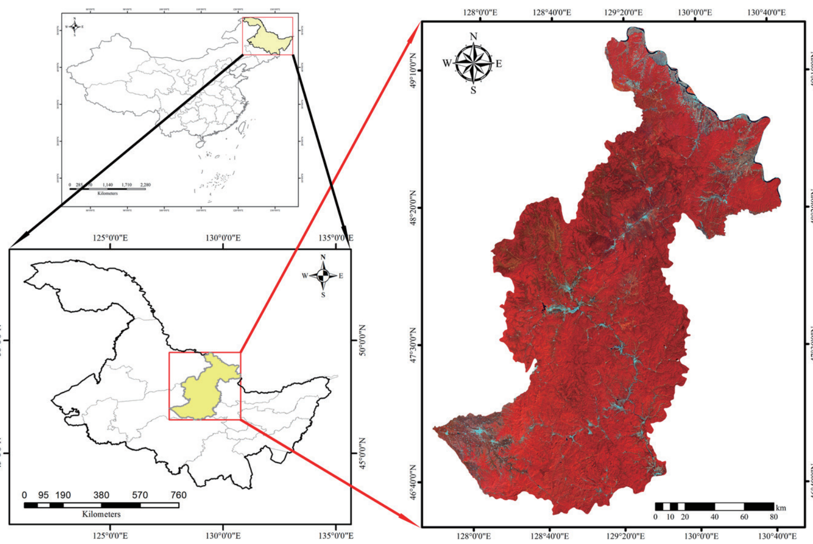


Fig. 1. (Color online) Overview of the study area. The top left is a map of China. The red boundary (Yichun City) in the bottom left is the study area. The right color image is obtained with Sentinel-2A.

Sieb), dahurian larch (*Larix gmelinii* Kuzen), spruce (*Picea asperata* Mast), fir (*Abies fabri* Craib), mongolian scotch pine (*Pinus sylvestris* var. mongolica Litv), *Populus tremula* (*Populus davidiana* Dode), and white birch (*Betula platyphylla* Sukaczev).

## 2.2 Data and preprocessing

### 2.2.1 Field data

The field data (Fig. 2) were acquired from forest inventory data in 2014. The survey included forest resources and a few stand characteristics, such as diameter at breast height (DBH), stocking volume, height, longitude, latitude, and tree species. A total of 728 forest plots (20 × 20 m$^2$) were used, including 40 white birch (*B. platyphylla* Sukaczev; BESU), 175 Korean pine (*P. koraiensis* Sieb; PISI), 43 fir (*A. fabri* Craib; ABCR), 241 dahurian larch (*L. gmelinii* Kuzen; LAKU), 41 *Populus tremula* (*P. davidiana* Dode; PODO), and 188 spruce (*P. asperata* Mast; PIMA).

### 2.2.2 MODIS data

MODIS is widely applied to estimate vegetation ecological parameters such as LAI, fractional vegetation cover (FVC), and GPP because of its abundant spectrum information, high time resolution, and excellent instrument properties.[12] In this study, the LAI and FVC were used to simulate the forest NPP, and the GPP values used for model validation were mainly obtained using MODIS products (MOD15 A2H, MOD44B, and MOD17A2H). The LAI was estimated on

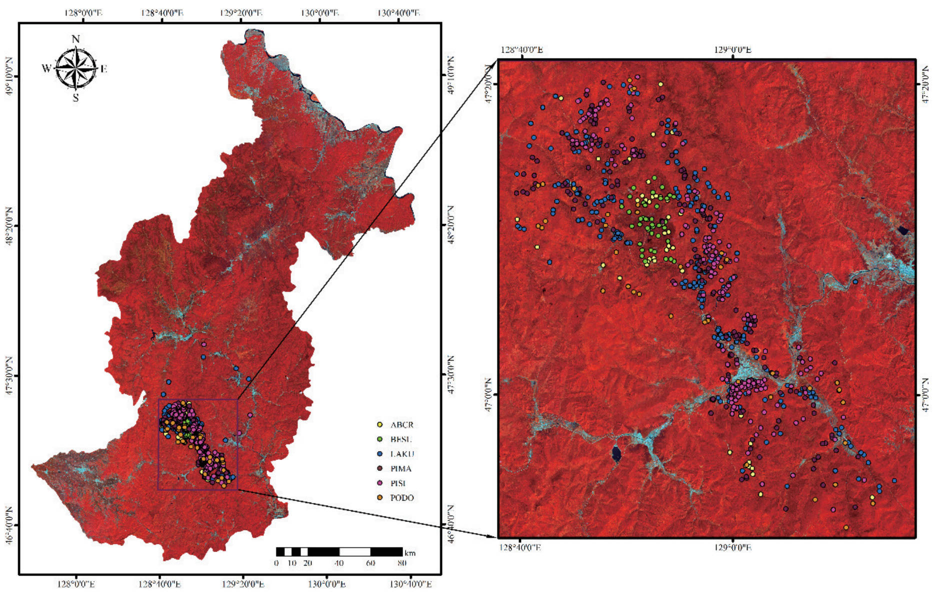


Fig. 2. (Color online) Field data map of the study area.

the basis of the radiation transfer model using MODIS reflectivity data and biome type maps. If the algorithm fails in the estimation process, an alternate algorithm is selected; that is, the LAI is calculated from the empirical relationship between the LAI and the normalized differential vegetation index (NDVI) for a specific land cover type. This product can simulate a scene in a forest ecosystem using a radiation transfer model and considers the impact on spatial heterogeneity inside the forest canopy. Therefore, NDVI provides high accuracy and reliability in simulating the LAI in a forest ecosystem.(13,14) A total of 15 MODIS LAI products, obtained for the period of March 31, 2017 to November 2, 2017 with 8-day temporal resolution and 500 m spatial resolution, were used in this study. To match the forest plot survey data, LAI products were resampled into images with a spatial resolution of $20 \times 20$ m$^2$. As the estimated data of the forest vegetation coverage ratio, the MODIS forest coverage product (MOD44B) was estimated using a classification and regression tree based on multi-temporal matrices in one year, with a root mean square error (RMSE) of approximately 9.06% in the quality report. One MODIS-FVC product, obtained on March 7, 2017 at a spatial resolution of 200 m, was downloaded for this study. This product was resampled to a spatial resolution of $20 \times 20$ m$^2$ to match the forest plot survey data. The MODIS GPP product (MOD17A2H) is the accumulated 8-day GPP value estimated with the light energy utilization model using the photosynthetically active radiation ratio data obtained from meteorological and remote sensing data, with a spatial resolution of 500 m. In this study, 25 MODIS GPP products were downloaded for the period of April 8, 2017 to October 25, 2017. These products were also resampled to a spatial resolution of $20 \times 20$ m$^2$ and used as reference data to verify the reliability of the NPP simulated using the physiological principles predicting growth (3-PG) model.

#### 2.2.3 Soil data

The mineral and organic matter content of the soil directly affects the photosynthetic rate of forest vegetation, in addition to the soil water content and other environmental factors. In the 3-PG model, data on soil properties mainly include information on soil fertility and water content. Soil fertility is mainly based on the modified Nemerow composite index method, and the fertility class of soil is calculated using the nitrogen, phosphorus, potassium, and organic matter contents of the soil. Soil water content was mainly obtained by calculating the average monthly humidity, temperature, and rainfall, and the average rainfall in the previous month.

#### 2.2.4 Meteorological data

The climatic data required for forest estimation were obtained from 81 meteorological stations in Heilongjiang Province, which includes the mean daily total solar radiation, mean temperature and saturation vapor pressure difference (VPD), monthly rainfall, and frost days. The actual monthly meteorological data and monthly average data from long-term observations were used in the 3-PG model. In this study, meteorological data were spatially interpolated using Kriging interpolation based on the geographic coordinate of a meteorological station. The geometric spatial distribution of meteorological stations is presented in Fig. 3.

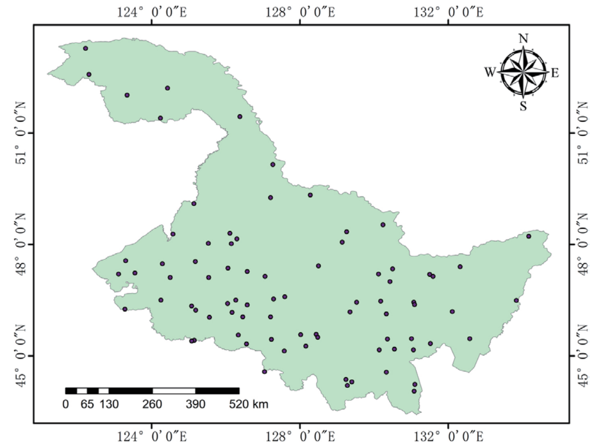


Fig. 3. (Color online) Geometric spatial distribution of meteorological stations in Heilongjiang province.

## 3. Method

The proposed methodological framework for NPP estimation is described in Fig. 4. For the forest NPP estimation, a 3-PG model driven by remote sensing data was established with LAI, FVC, soil fertility, water content, mean daily total solar radiation, mean temperature and saturation VPD, monthly rainfall, and frost days. Then model evaluation was carried out using the NPP derived from MODIS. Moreover, the analysis was developed from monthly variations in NPP and related influencing factors.

### 3.1 NPP estimation model

The 3-PG model, the most widely used process-based growth model,[15,16] is constructed with a set of well-established principles and certain fixed constants. The model can simulate the actual growth of forest stands with few parameters and obtain the required parameters combined with remote sensing data, enabling the estimation of forest growth in large areas.

Environmental factors were considered through multiplicative modifiers based on stand age, temperature, frost days per month, atmospheric vapor pressure deficit, available soil water, and soil nutrition in the 3-PG model, as tree productivity is affected by all these modifiers. Therefore, the input data of the model included meteorological, forest-field, and soil data, biophysical variables derived from remote sensing data, and parameters. To calculate the modifiers of temperature, frost, water pressure difference, and soil water content on photosynthesis, we collected monthly meteorological data, such as frost days, maximum, average, and minimum temperatures, total precipitation, and average humidity. In this study, the modifier of site nutrition was calculated from the nitrogen, phosphorus, and potassium contents and soil organic matter. The age modifier was calculated on the basis of stand age derived from forest inventory data.

The 3-PG model includes a specific set of parameters for each tree species. In this study, all these parameters (Tables 1 and 2) were determined using the same or similar tree species from

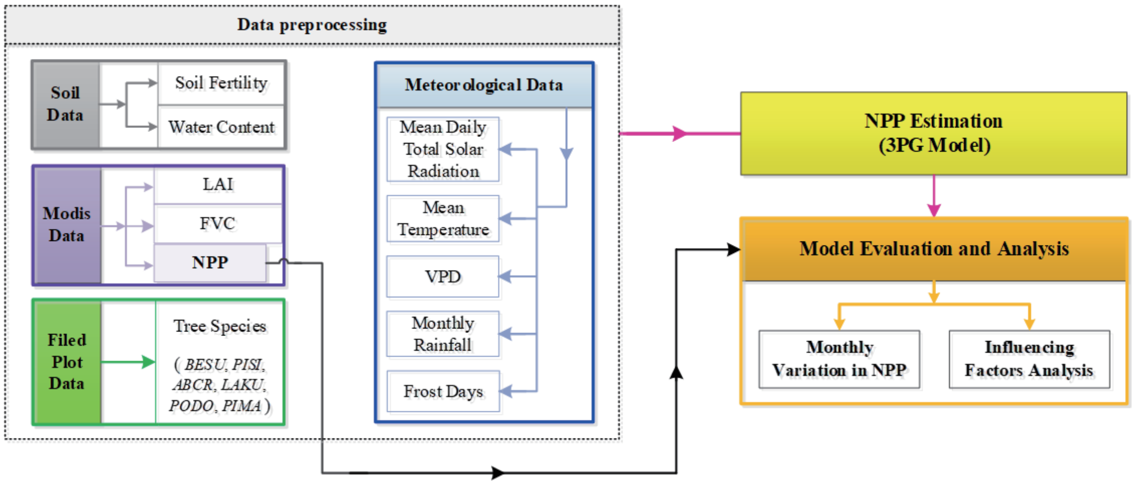


Fig. 4. (Color online) Methodological framework for forest NPP estimation.

Table 1
Parameters used in this study.

| Parameter description | Symbol | Unit |
|---|---|---|
| Extinction coefficient for absorption of Photosynthetically Active Radiation (PAR) by canopy | $k$ | — |
| Maximum canopy quantum efficiency | $\alpha Cx$ | molC/molPAR |
| Minimum temperature for growth | *Tmin* | °C |
| Optimum temperature for growth | *Topt* | °C |
| Maximum temperature for growth | *Tmax* | °C |
| Days production lost per frost day | *kF* | days |
| Value of $f_{N0}$ when $FR = 0$ | *fN0* | — |
| Value of $nf_N$ when $FR = 0$ | *nfN* | — |
| Defines stomatal response to VPD | *kD* | 1/mBar |
| Maximum stand age used in age modifier | *MaxAge* | years |
| Power of relative age in function for $f_{age}$ | $n_{age}$ | — |
| Relative age to give $f_{age} = 0.5$ | $r_{age}$ | — |

Table 2
Parameter values in 3-PG for six typical tree species.

| Parameter description | Tree species | | | | | |
|---|---|---|---|---|---|---|
| | LAKU | PIMA | ABCR | PISI | PODO | BESU |
| Extinction coefficient for absorption of PAR by canopy ($k$) | 0.5 | 0.5 | 0.5 | 0.52 | 0.779 | 0.565 |
| Maximum canopy quantum efficiency ($\alpha Cx$) molC/molPAR | 0.05 | 0.06 | 0.06 | 0.05 | 0.08 | 0.012 |
| Minimum temperature for growth ($T_{min}$/°C) | −2 | −5 | −5 | −5 | 10 | 8.5 |
| Optimum temperature for growth ($T_{opt}$/°C) | 17 | 12 | 12 | 15 | 30 | 24.5 |
| Maximum temperature for growth ($T_{max}$/°C) | 38 | 35 | 35 | 35 | 48 | 36 |
| Days production lost per frost day ($kF$) | 1 | 1 | 1 | 1 | 1 | 1 |
| Value of $f_{N0}$ when $FR = 0$ | 1 | 0.3 | 0.3 | 0.6 | 0.26 | 1 |
| Value of $nf_N$ when $FR = 0$ | 1 | 1 | 1 | 1 | 1 | 0 |
| Defines stomatal response to VPD ($kD$) 1/mBar | 0.05 | 0.05 | 0.05 | 0.05 | 0.05 | 0.05 |
| Maximum stand age used in age modifier ($MaxAge$) years | 300 | 300 | 300 | 300 | 0.05 | 0.05 |
| Power of relative age in function for $f_{age}$ ($n_{age}$) | 4 | 4 | 4 | 4 | 4 | 4 |
| Relative age to give $f_{age} = 0.5$ ($r_{age}$) | 0.95 | 0.95 | 0.95 | 0.75 | 0.95 | 0.95 |
| Extinction coefficient for absorption of PAR by canopy ($k$) | 0.5 | 0.5 | 0.5 | 0.52 | 0.779 | 0.565 |
| Maximum canopy quantum efficiency ($\alpha Cx$) molC/molPAR | 0.05 | 0.06 | 0.06 | 0.05 | 0.08 | 0.012 |

previous studies. The parameters included biomass distribution and turnover, as well as temperature, frost, soil fertility, and vapor pressure deficit modifiers.

### 3.2 Model evaluation

The MODIS GPP and previous research results were used to evaluate the performance of the 3-PG model based on remote sensing data. Studies demonstrated the effectiveness of MODIS GPP products in most plant communities.(17) The results were assessed by comparing the predicted values with the NPP derived from the MODIS GPP product, using the determination coefficient ($R^2$). Additionally, the results of previous studies were used for further evaluation and analysis.

## 4. Results

### 4.1 Accuracy assessment of NPP estimation

In this study, the GPP of six typical tree species was estimated using a 3-PG model driven by remote sensing data. Combined with the spatial geographical coordinates of the sample plots, the estimated GPP value derived from 3-PG and that from mod17a2 in the corresponding sample plot geospatial area were extracted using ArcGIS software. A study(18) has revealed that the ratio of NPP to GPP for trees is approximately 0.5. Therefore, GPP was converted to NPP on the basis of this ratio coefficient in this study. The NPP estimation results are presented in Table 3.

As shown in Table 3, the NPP value of BESU estimated with the 3-PG model ranges from 4.11 to 7.97, with an average of 6.79, whereas that derived from the MODIS product ranges from 3.60 to 4.78, with an average of 4.18. The comparison reveals that NPP derived from MODIS is underestimated. The PISI NPP value estimated with the 3-PG model ranges from 2.39 to 6.15, with an average of 4.37, whereas that acquired from the MODIS product ranges from 3.47 to 4.98, with an average of 4.24. Although the NPP mean value estimated with the 3-PG model differed only slightly from that derived from the MODIS products, the NPP value range

Table 3
Results of NPP estimated using 3-PG and derived using MODIS product.

| Tree species | NPP | Mean ($t{\cdot}ha^{-1}{\cdot}a^{-1}$) | Max ($t{\cdot}ha^{-1}{\cdot}a^{-1}$) | Min ($t{\cdot}ha^{-1}{\cdot}a^{-1}$) |
|---|---|---|---|---|
| BESU | 3-PG | 6.79 | 7.97 | 4.11 |
| | MODIS | 4.18 | 4.78 | 3.60 |
| PISI | 3-PG | 4.37 | 6.15 | 2.39 |
| | MODIS | 4.24 | 4.98 | 3.47 |
| ABCR | 3-PG | 4.97 | 6.93 | 3.02 |
| | MODIS | 4.21 | 4.59 | 3.75 |
| LAKU | 3-PG | 6.12 | 9.37 | 2.70 |
| | MODIS | 4.36 | 5.49 | 3.71 |
| PODO | 3-PG | 9.17 | 12.00 | 5.67 |
| | MODIS | 4.49 | 5.20 | 3.93 |
| PIMA | 3-PG | 4.99 | 6.96 | 1.93 |
| | MODIS | 4.24 | 5.12 | 3.29 |

estimated with the 3-PG model was slightly larger than that from the MODIS products. For ABCR and PIMA, which belong to the Pinaceae evergreen tree family, the NPP values estimated with the 3-PG model range from 3.02 to 6.93 and 1.93 to 6.96, respectively, with respective mean values of 4.97 and 4.99, whereas the NPP values estimated with the MODIS product range from 3.75 to 4.59 and 3.29 to 5.12, respectively, with respective mean values of 4.21 and 4.24. The NPP value range derived from the MODIS product was smaller with a lower mean. For LAKU, the NPP estimated with the 3-PG model ranges from 2.70 to 9.37, with an average of 6.12, whereas the same derived from the MODIS product ranges from 3.71 to 5.49 with an average of 4.36. The NPP values for PODO estimated with the 3-PG model ranged from 5.67 to 12.00 with an average of 9.17, whereas those from MODIS ranged from 3.93 to 5.20 with an average of 4.49. It can be observed that the NPP of PODO derived from MODIS products is underestimated.

To further verify the reliability of the 3-PG model in estimating the NPP of six typical tree species in Northeast China, the correlation between NPP values estimated with the 3-PG model and those derived from the MODIS product was calculated, as illustrated in Fig. 5. As evident from Fig. 5, there is an excellent correlation between the NPP values estimated with the 3-PG model and MODIS product. PODO, ABCR, and BESU exhibit the highest correlation coefficients of 0.5462, 0.4793, and 0.4434, respectively. This is followed by PISI, PIMA, and LAKU, with correlation coefficients ranging from 0.4010 to 0.4073. The NPP value estimated with the 3-PG model was higher than that from the MODIS product, which may be attributable to the difference in the data source or data acquisition time between the MODIS product and the NPP estimation.

To further illustrate the reliability of the NPP estimation, the NPP values estimated with the 3-PG model and those from previous studies were comparatively analyzed. Li *et al.*(19) simulated the NPP of ABCR in Miyaluo, Sichuan, for the period of 1954 to 2008 using the BIOME-BGC model and obtained values ranging from 4.99 to 5.64, with an average of 5.27. Hong(20) studied the NPP of PIMA natural stands and obtained an average NPP of 5.66. The average NPPs of ABCR and PIMA estimated with the 3-PG model in this study were 4.97 and 4.99, respectively, which are similar to the existing research results. Headlee *et al.*(21) estimated the NPP of PODO in Minnesota and Wisconsin, USA, using the 3-PG model and obtained values ranging from 4.4 to 13.0, and an approximate average NPP of 8.15 for PODO in a Wawushan forest farm was obtained using an improved CASA model with Landsat TM imagery, meteorological data, and forest inventory data. The NPP value of PODO estimated in this study ranged from 5.67 to 11.99, with an average of 9.17. It is evident that the PODO NPP results in this study are reasonable. Xie *et al.*(22) estimated the NPP of LAKU using the 3-PG model; the values ranged from 2.73 to 8.45, with an average of 5.78. This is similar to the estimates of LAKU NPP in this study. Wu *et al.*(23) obtained a simulated NPP range of 4.73–7.03 for broad-leaved PISI in Changbai Mountains using the BIOME-BGC model, with an average of 6.12. The NPP values for PISI estimated in this study ranged from 2.36 to 6.15, with an average of 4.73, which are lower than those estimated in a previous study because broad-leaved PISI is a mixed forest of coniferous and broad-leaved forests. The average NPP of BESU estimated was 6.28, similar to the NPP of the BESU estimated in this study.(24)

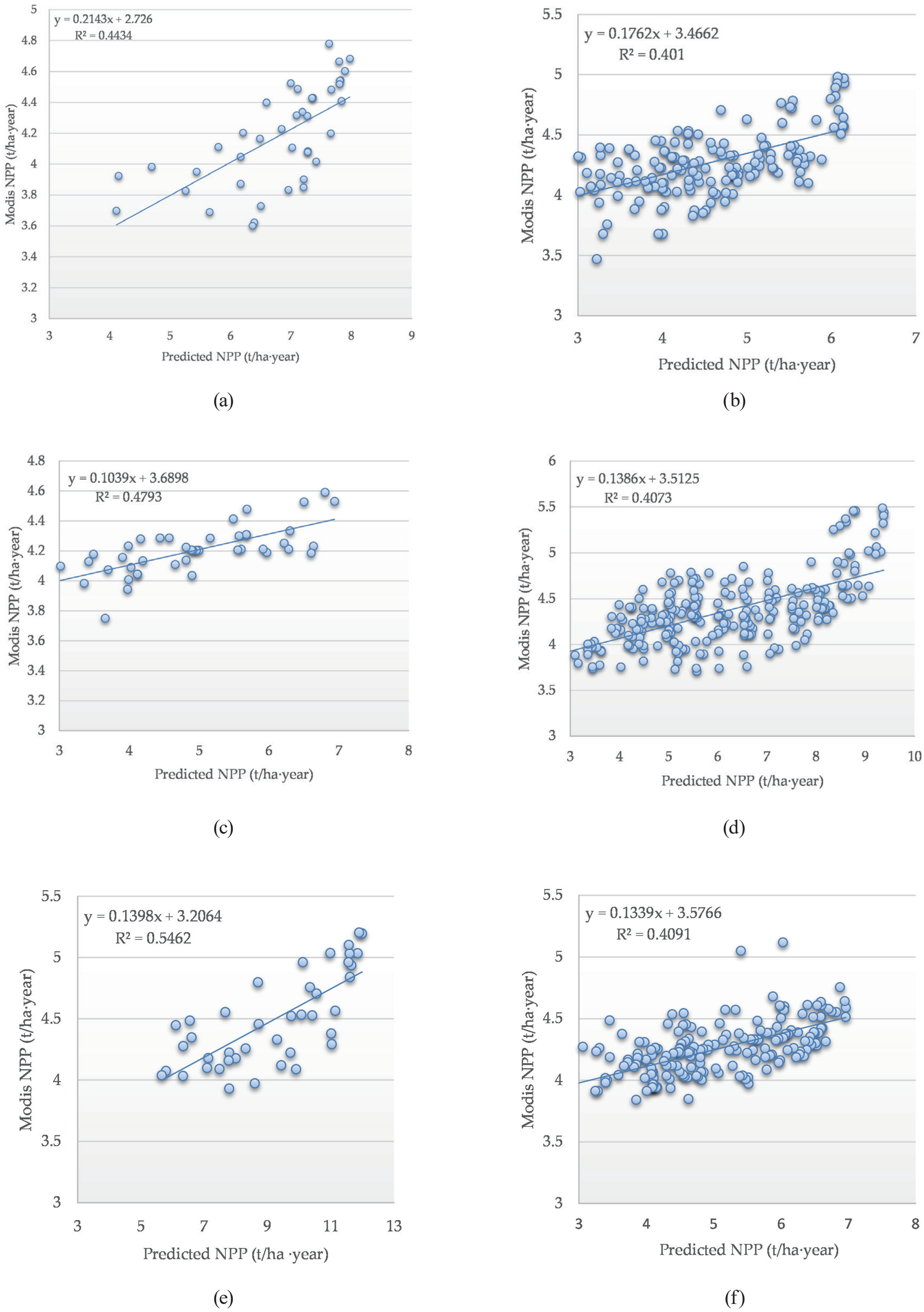


Fig. 5. (Color online) Correlation between predicted NPP vs MODIS NPP for six typical tree species. (a) *B. platyphylla* Sukaczev, BESU. (b) *P. koraiensis* Sieb, PISI. (c) *A. fabri* Craib, ABCR. (d) *L. gmelinii* Kuzen, LAKU. (e) *P. davidiana* Dode, PODO. (f) *P. asperata* Mast, PIMA.

### 4.2 Monthly variation in NPP for six typical tree species

The forest vegetation does not perform any photosynthesis in the 3-PG model when the ground temperature drops below 0 °C.[16] According to the meteorological data of the study area, it can be concluded that the forest vegetation growth period begins in early May and ends in late September. Therefore, the forest NPP was zero from January to April and from October to December. Figure 6 illustrates the variation in forest NPP from January to December.

As depicted in Fig. 6, the monthly NPP variation trends are consistent from January to December, first increasing, reaching the maximum value, and then decreasing gradually. Because the ground temperature dropped below 0 °C from October to April of the following year, the NPP was 0. The NPP gradually increased from May, reached a maximum around July, and then gradually decreased until it reached zero in October. Additionally, it can be observed that the monthly NPP for broad-leaved forests (PODO and BESU) is greater than that for coniferous forests (LAKU, PISI, PIMA, and ABCR). PODO exhibited the highest monthly NPP of 4.73 in July, followed by 3.53 of BESU in July. The lowest monthly NPP values of 1.89, 1.90, and 1.94 were observed for ABCR, PIMA, and PISI, respectively.

### 4.3 Analysis of factors influencing monthly variation in forest NPP

In the 3-PG model, the environmental factors affecting the photosynthesis of forest vegetation mainly include temperature, frost days per month, soil nutrition, atmospheric vapor pressure deficit, available soil water, and stand age. The growth period of forest vegetation was mainly concentrated from May to September. Therefore, the impact of environmental factors on the monthly variation in forest NPP during this period was analyzed. The frost-free period at the study site is also mainly concentrated from May to September; therefore, the frost in this period has no effect on the growth of forest vegetation, that is, the value is 1. Owing to the small differences in soil types and meteorological conditions within the geographic region where the sample plot data were located, the differences between the growth modifiers of available soil

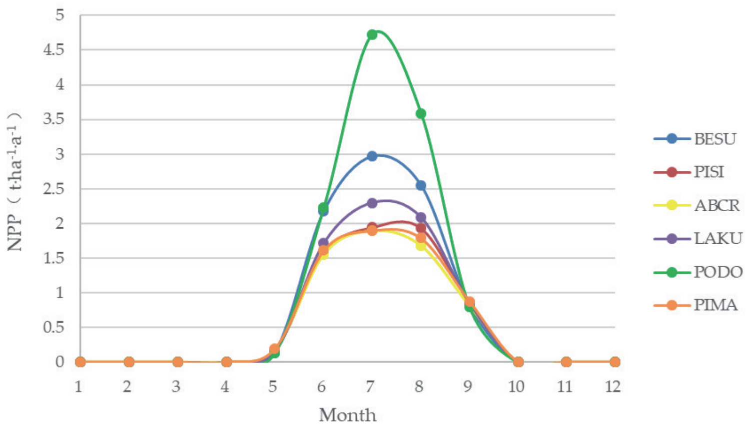


Fig. 6. (Color online) NPP of six typical tree species from January to December.

water and atmospheric vapor pressure deficit for different forest types were small. The average values of available soil water and atmospheric vapor pressure deficit in different forest types were analyzed.

As illustrated in Fig. 7, the value of available soil water mainly ranges between 0.0468 and 0.1752 and is a factor limiting forest growth. The value in May had the strongest influence on limiting the forest growth. In Fig. 8, the value of the atmospheric vapor pressure deficit mainly ranges from 0.9488 to 0.9679, indicating that it has little effect on the photosynthesis of forest vegetation at the study site. The growth temperature is different for different forest types; therefore, the effect of temperature on photosynthesis for different forest types is also different.

As illustrated in Fig. 9, the effects of temperature on photosynthesis in broad-leaved (BESU and PODO) and coniferous (PISI, ABCR, LAKU, and PIMA) forests are quite different from May to September. The effect of temperature on the photosynthetic production of broad-leaved forests gradually decreases from May, is the smallest between July and August, and then gradually increases. In addition, temperature has a greater impact on the photosynthetic production of poplar than that of birch. The effect of temperature on the photosynthetic production of coniferous forests gradually increases from May, reaches a maximum between July and August, and then gradually decreases. Overall, low temperature has a greater impact on the photosynthetic production of broad-leaved forests, and high temperature has a greater impact on the photosynthetic production of coniferous forests. Figure 10 depicts the age growth modifiers for these forest types.

As illustrated in Fig. 10, the values of age growth modifiers are mainly distributed between 0.9496 and 0.9998, indicating that age has little effect on photosynthetic production for different forest types at the study site. In addition, in Fig. 11, the values of soil nutrition growth modifiers are mainly distributed between 0.8526 and 1, which demonstrates that soil nutrition has a certain effect on the photosynthetic production of ABCR, PODO, and PIMA, but less of an effect on the photosynthetic production of other forest types.

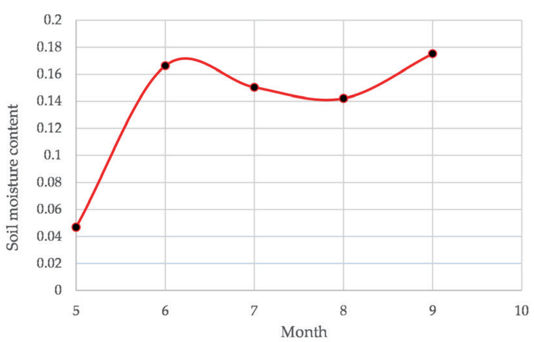


Fig. 7. (Color online) Map of soil moisture content for different months.

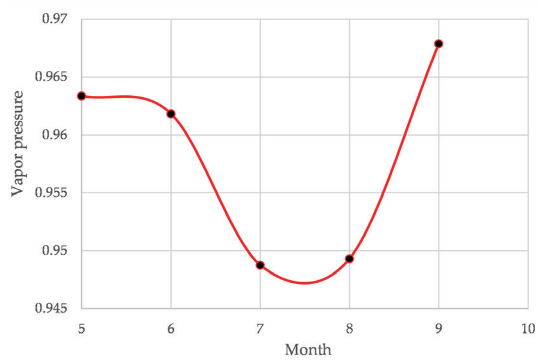


Fig. 8. (Color online) Vapor pressure map for different months.

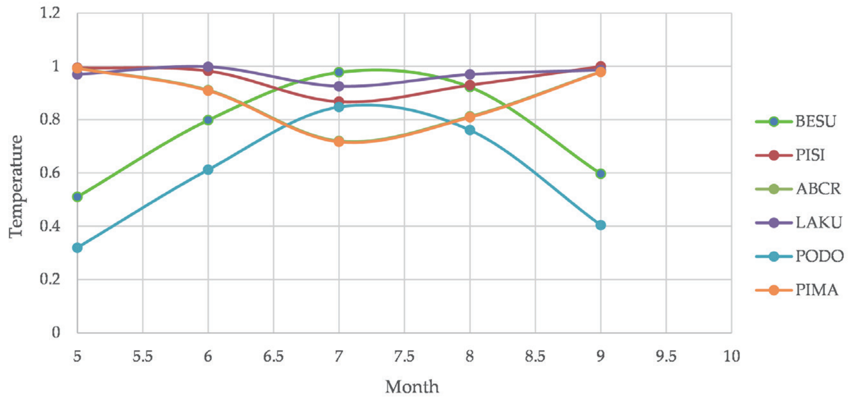


Fig. 9. (Color online) Temperature map for different months.

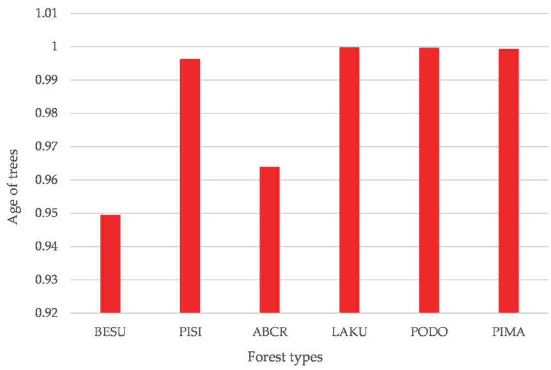


Fig. 10. (Color online) Age growth modifiers for different forest types.

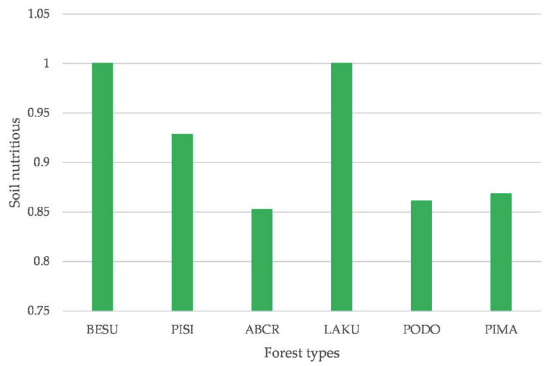


Fig. 11. (Color online) Soil nutrients of different forest types.

## 5. Discussion

The 3-PG model has been widely used to estimate the NPP of different forest types.(25) However, few groups have simultaneously applied the model to estimate NPP for multiple forest types in Northeast China. In this study, a 3-PG model based on remote sensing data was explored to estimate the NPP of six forest types in Northeast China and highly reliable estimates were obtained.

The development and application of coupling process models with remote sensing have been greatly promoted to provide the richness and easy transformation of spatial scales in remote sensing data. To fully utilize remote sensing data in simplifying the complex forest growth process mechanism model and estimating large-scale forest NPP, a method based on the coupling 3-PG model with remote sensing was proposed in this study. Ecological parameters derived from remote sensing data were used as the input of the 3-PG model to estimate the NPP of different forest types. The reliability of the model was verified by comparing the results of the

NPP estimation in this study with the corresponding MODIS NPP products and the results of similar research studies.

The forest NPP formation process is extremely complex and is affected by several factors, including the physiological and ecological factors of the forest vegetation itself, as well as a large number of complex environmental factors, such as soil and climate. In reality, incorporating all environmental factors and ecological and physiological processes into the NPP estimation model is difficult at a regional or global scale. Generally, simplification of the entire forest's ecological and physiological processes results in differences between the simulated results and the real values. Currently, dozens of NPP estimation models are available, and the estimation results vary greatly in spatial distribution and value.(26) The input and control parameters are frequently different in different NPP estimation models. Even for consistent input and control parameters, the estimation results vary significantly with different model algorithms, input data sources, and spatial resolutions. In addition, GPP is closely coupled with land surface energy and water cycles through vegetation stomatal controls. Therefore, uncertainties of land energy/water/carbon cycles originating from the model structure, input data, and model parameterizations can all affect GPP or NPP estimation.(27–30) For example, the NPP estimation results obtained by different researchers can vary by nearly eight times in China. Simultaneously, most NPP model verification methods are comparative analyses of estimation results, and there is no unified on appropriate verification method, which is an important research direction in the future.(8)

An uncertainty analysis for NPP estimates was performed because of a few uncertainties observed in the NPP estimation results when using the process-based model. Uncertainty mainly originates from several aspects, such as sample plot data, model method, input parameters, and spatial scale expansion. The uncertainty of the sample plot data can be caused by measurement errors in forest age, tree height, or DBH during the field survey. The errors mainly arise from the differences in the accuracies of the measurement instruments, measurement conditions of the sample plot, or human factors. Different models consider different structures and applicable conditions and produce different accuracies during NPP estimation. Therefore, there is a difference between the estimation results obtained from the 3-PG model and the MODIS product. The reliability and accuracy of the NPP estimation model depend on an in-depth understanding and mastery of the physiological and ecological processes of vegetation. Reliable estimation results can be obtained via parameter calibration and model simplification. The data sources of the 3-PG model included meteorological data, soil data, forest type attribute data, and LAI derived from remote sensing data. The source, consistency, precision, reliability, and temporal and spatial scales of these data all have an impact on the NPP estimation results.

Most studies have focused on the NPP estimation of one tree species or forest type, and few have concentrated on estimating the NPP for multiple forest types. In this study, the monthly NPP variation for six typical tree species was determined. The trends of NPP monthly variation for the six typical tree species were similar because they are related to climatic conditions and the natural environment of the study site. Overall, the NPP of broad-leaved forests was greater than that of coniferous forests, which is consistent with the research results.(31) PODO had the highest NPP among the six typical tree species. Comparative analysis of the monthly forest NPP variation can provide guidance for forest resources management and ecological construction.

An analysis of the factors affecting the monthly variation in forest NPP at the study site can provide a basis for forest resource management. Most studies have been concentrated on analyzing the impact of environmental factors on an annual scale or in different seasons between years, and few studies have been on the analysis of the impact of environmental factors on a monthly time scale. In this study, we analyzed the impact of environmental factors on forest NPP and found with temperature and available soil water to exert the greatest impact on forest NPP, consistent with the observations.(32)

## 6. Conclusions

The mechanism of the ecological-process-based model is complex and involves several input parameters, affecting its popularization and application over a large area. Taking into consideration the rich information provided by remote sensing data can simplify the estimation model and allow better transformation of the spatial scale. In this study, a remote sensing-3-PG process coupling model was proposed, which can efficiently and reliably estimate NPP at the regional scale and provide data support for understanding the carbon balance of ecosystems at the national/regional scales and for responding to global climate change. Different geographical environments for the same forest type may lead to differences in input parameters when estimating forest NPP. The parameters of the 3-PG models for different forest types used in this study were obtained from existing research results. Therefore, further research is required to estimate the input parameters of different forests types in different areas for optimizing the parameters and NPP estimation results.

## Acknowledgments

We thank the anonymous reviewers for their assistance, and we would like to thank Editage (www.editage.cn) for English language editing. This work was jointly supported by the National Natural Science Foundation of China (Grant Number, 42001379), the Fundamental Research Funds for Beijing University of Civil Engineering and Architecture (Grant Number, X22024, Y2207), and the Pyramid Talent Training Project for Beijing University of Civil Engineering and Architecture (Grant Number, JDYC20220824).

## References

1 Y. Pan, R. A. Birdsey, J. Fang, R. Houghton, P. E. Kauppi, W. A. Kurz, O. L. Phillips, A. Shvidenko, S. L. Lewis, J. G. Canadell, P. Ciais, R. B. Jackson, S. W. Pacala, A. D. McGuire, S. Piao, A. Rautiainen, S. Sitch, and D. Hayes: Science **333** (2011) 988. http://dx.doi.org/10.1126/science.1201609
2 H. Lieth: Modeling the Primary Productivity of the World: In Primary Productivity of the Biosphere (Springer Berlin Heidelberg, Berlin, Heidelberg, 1975) p. 237.http://dx.doi.org/10.1007/978-3-642-80913-2_12
3 B. Field Christopher, J. Behrenfeld Michael, T. Randerson James, and P. Falkowski: Science **281** (1998) 237. http://dx.doi.org/10.1126/science.281.5374.237
4 Z. Uchijima and H. Seino: J. Agric. Meteorol. **40** (1985) 343. https://doi.org/10.2480/agrmet.40.343
5 W. Gong, C. Huang, R. A. Houghton, A. Nassikas, F. Zhao, X. Tao, J. Lu, and K. Schleeweis: Sci. Remote Sens. **5** (2022) 100042. https://doi.org/10.1016/j.srs.2022.100042
6 M. K. Hazarika, Y. Yasuoka, A. Ito, and D. Dye: Remote Sensi. Environ. **94** (2005) 298. https://doi.org/10.1016/j.rse.2004.10.004

7 Y. Zhou, B. Xing, and W. Ju: IEEE J. Sel. Top. Appl. Earth Obs. Remote Sens. **8** (2015) 2318. http://dx.doi.org/10.1109/JSTARS.2015.2440274
8 S. Li, Z. Niu, and B. Li: Res. Soil Water Conserv. **3** (2005) 126. https://doi.org/10.3969/j.issn.1005-3409.2005.03.041
9 R. Zhang, Y. Zhou, H. Luo, F. Wang, and S. Wang: Remote Sens. **9** (2017) 477. https://doi.org/10.3390/rs9050477
10 C. D. Keeling, J. F. S. Chin, and T. P. Whorf: Nature **382** (1996) 146. http://dx.doi.org/10.1038/382146a0
11 S. S. Saatchi, N. L. Harris, S. Brown, M. Lefsky, E. T. Mitchard, W. Salas, B. R. Zutta, W. Buermann, S. L. Lewis, and S. Hagen: Proc. National Academy of Sciences **108** (2011) 9899. http://dx.doi.org/10.1073/pnas.1019576108
12 P. C. Doraiswamy, T. R. Sinclair, S. Hollinger, B. Akhmedov, A. Stern, and J. Prueger: Remote Sens. Environ. **97** (2005) 192. https://doi.org/10.1016/j.rse.2005.03.015
13 F. Camacho, J. Cernicharo, R. Lacaze, F. Baret, and M. Weiss: Remote Sens. Environ. **137** (2013) 310. https://doi.org/10.1016/j.rse.2013.02.030
14 D. Huang, Y. Knyazikhin, W. Wang, D. W. Deering, P. Stenberg, N. Shabanov, B. Tan, and R. B. Myneni: Remote Sens. Environ. **112** (2008) 35. https://doi.org/10.1016/j.rse.2006.05.026
15 R. H. Waring, N. C. Coops, and S. W. Running: Remote Sens. Environ. **115** (2011) 3554. https://doi.org/10.1016/j.rse.2011.08.017
16 J. J. Landsberg and R. H. Waring: For. Ecol. Manage. **95** (1997) 209. https://doi.org/10.1016/S0378-1127(97)00026-1
17 M. Jung, M. Reichstein, H. A. Margolis, A. Cescatti, A. D. Richardson, M. A. Arain, A. Arneth, C. Bernhofer, D. Bonal, and J. Chen: J. Geophys. Res.: Biogeosciences **116** (2011). http://dx.doi.org/ https://doi.org/10.1029/2010JG001566
18 B. Law, M. Williams, P. Anthoni, D. Baldocchi, and M. Unsworth: Global Change Biol. **6** (2000) 613. http://dx.doi.org/ https://doi.org/10.1046/j.1365-2486.2000.00339.x
19 Z. Li, G. Liu, X. Wu, L. Gong, M. Wang, and J. Peng: Quat. Sci. **34** (2014) 830. https://doi.org/10.3969/j.issn.1001-7410.2014.04.16
20 J. Hong: J. Integr. Plant Biol. **28** (1986). https://www.jipb.net/EN/abstract/abstract27259.shtml (accessed December 2022)
21 W. L. Headlee, R. S. Zalesny, D. M. Donner, and R. B. Hall: BioEnergy Res. **6** (2013) 196. https://doi.org/10.1007/s12155-012-9251-x
22 Y. Xie, H. Wang, and X. Lei: Chin. J. Plant Ecolog. **41** (2017) 826. https://doi.org/10.17521/cjpe.2016.0382
23 Y. Wu, X. Wang, Q. Li, and S. Yan: Acta Scientiarum Naturalium Universitatis Pekinensis **50** (2014) 577 (in Chinese). https://doi.org/10.13209/j.0479-8023.2014.077
24 S. Potithep and Y. Yasuoka: Forests **2** (2011). https://doi.org/10.3390/f2020590
25 Y. Xie, H. Wang, and X. Lei: For. Ecol. Manage. **406** (2017) 208. https://doi.org/10.1016/j.foreco.2017.10.018
26 W. Cramer, D. W. Kicklighter, A. Bondeau, B. M. Iii, G. Churkina, B. Nemry, A. Ruimy, A. L. Schloss, and ThE Participants OF ThE Potsdam NpP Model Intercomparison: Global Change Biol. **5** (1999) 1. https://doi.org/10.1046/j.1365-2486.1999.00009.x
27 G. Wu, X. Cai, T. F. Keenan, S. Li, X. Luo, J. B. Fisher, R. Cao, F. Li, A. J. Purdy, W. Zhao, X. Sun, and Z. Hu: J. Hydrol. **590** (2020) 125553. https://doi.org/10.1016/j.jhydrol.2020.125553
28 F. Li, D. Hao, Q. Zhu, K. Yuan, R. K. Braghiere, L. He, X. Luo, S. Wei, W. J. Riley, Y. Zeng, and M. Chen: Global Change Biol. **29** (2022) 731. https://doi.org/10.1111/gcb.16503
29 K. Yuan, Q. Zhu, W. J. Riley, F. Li, and H. Wu: Agric. For. Meteorol. **319** (2022) 108920. https://doi.org/10.1016/j.agrformet.2022.108920
30 K. Yuan, Q. Zhu, S. Zheng, L. Zhao, M. Chen, W. J. Riley, X. Cai, H. Ma, F. Li, H. Wu, and L. Chen: Environ. Res. Lett. **16** (2021) 024014. https://doi.org/10.1088/1748-9326/abd8f9
31 X. Li, Y. Zheng, C. Wang, and Y. Yu: Chin. J. Agrometeorology **31** (2010) 88. https://doi.org/10.3969/j.issn.1000-6362.2010.01.018
32 W. Liu, X. Li, T. Li, and B. Jia: Chinese J. Ecology. **41** (2021) 150 (in Chinese). https://doi.org/10.13292/j.1000-4890.202201.026

## About the Authors

**Yanan Liu** received her Ph.D. degree from Wuhan University, China, in 2020. Her research interest mainly focuses on remote sensing applications. Her specific research directions include high-resolution remote sensing image processing and analysis, key technologies and applications for forest analysis, and remote sensing. (liuyanan@bucea.edu.cn)

**Peng Gao** received his B.S. degree from Beijing University of Civil Engineering and Architecture, China, in 2022, where he is currently pursuing his M.S. degree in photogrammetry and remote sensing. His research interests are in remote sensing and forest analysis. (2108570022088@stu.bucea.edu.cn)

**Dandan Liu** received her Ph.D. degree from Northeast Forestry University, China, in 2008. At present, she is a professor in the School of Civil and Architecture Engineering, Panzhihua University, and is mainly engaged in the teaching and research of surveying and geomatics. She has published more than 60 academic papers and four books. (1802363325@qq.com)

**Mengxue Xu** received her undergraduate degree from Beijing University of Civil Engineering and Architecture, China, in 2022, where she is currently pursuing her M.S. degree in photogrammetry and remote sensing. Her research interest is in remote sensing applications. (201804010301@stu.bucea.edu.cn)

**Yian Wang** is currently pursuing her B.S. degree at Beijing University of Civil Engineering and Architecture, China. Her major is remote sensing science and technology. (202003010214@stu.bucea.edu.cn)

**Ran Chen** entered the School of Surveying and Mapping at Beijing University of Civil Engineering and Architecture in 2020 and is currently pursuing her bachelor's degree in remote sensing science and technology. (202003010303@stu.bucea.edu.cn)